

Figure S1. Analysis of two forms of *ZC4H2*. A. Schematic of the genomic organization of the long (ENST00000374839; NM_018684) and short (ENST00000337990; NM_001178032) forms of *ZC4H2*. B. MTC Panel analysis. *ZC4H2* Long form = 838bp; *ZC4H2* short form = 606bp; *G3PDH* = 850bp. C. Rapid Scan Human Brain Panel analysis. *ZC4H2* Long form = 838bp; *ZC4H2* short form = 606bp; *GAPDH* = 151bp.

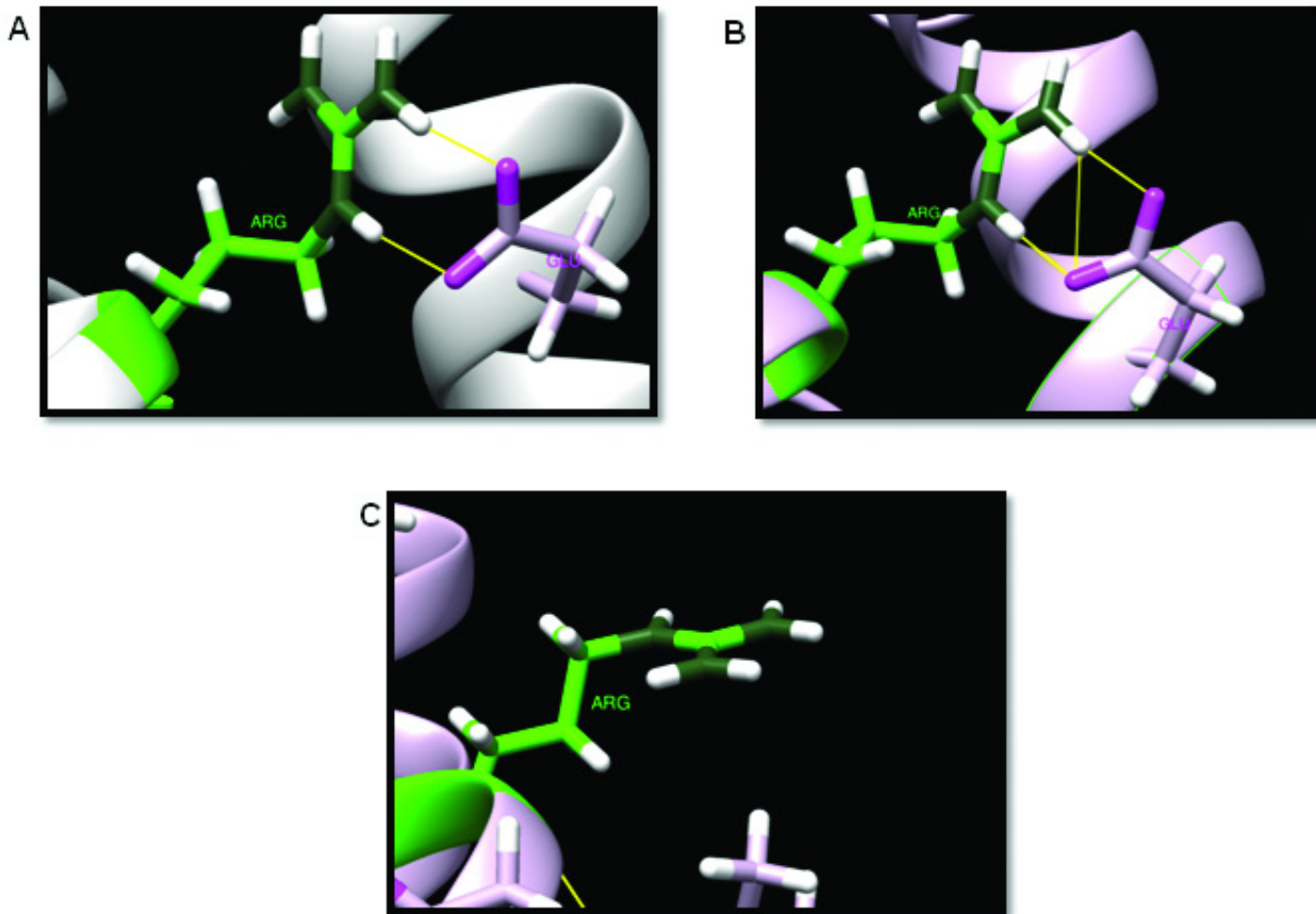


Figure S2. The hydrogen bond network of ARG18 in the WT structure models 2 and 3.

Two general cases are shown: (1) ARG18 making hydrogen bonds with neighboring residues and (2) ARG18 being completely exposed to the water phase. A illustrates the WT structure of model 2 analyzed using the Amber force field: ARG 18 (green) forms two hydrogen bonds with neighboring residue GLU 106 (light pink). B shows the WT structure of model 2 analyzed using the Charmm force field: ARG18 (green) forms three hydrogen bonds with GLU106 (light pink). C illustrates the WT structure of model 3 analyzed using the Amber force field: ARG18 (green) is completely exposed to the water phase and forms no hydrogen bonds with neighboring residues.

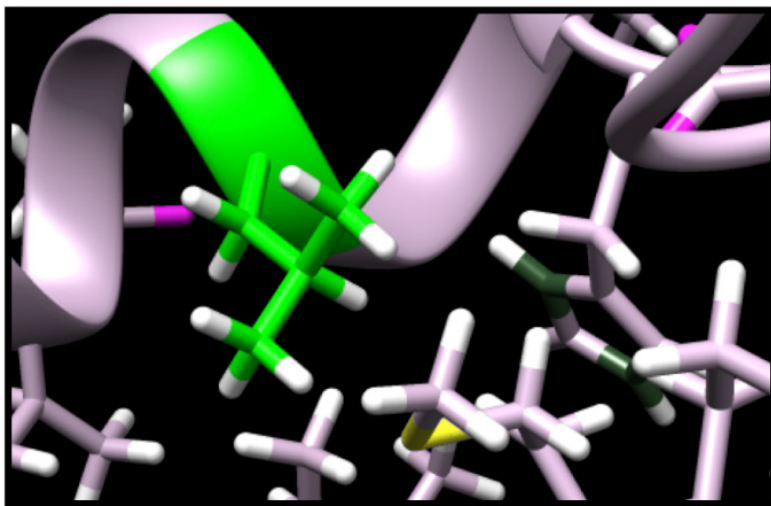


Figure S3. The WT structure analyzed using the Charmm force field. Residue LEU66 (green) is completely buried and surrounded by hydrophobic residues.

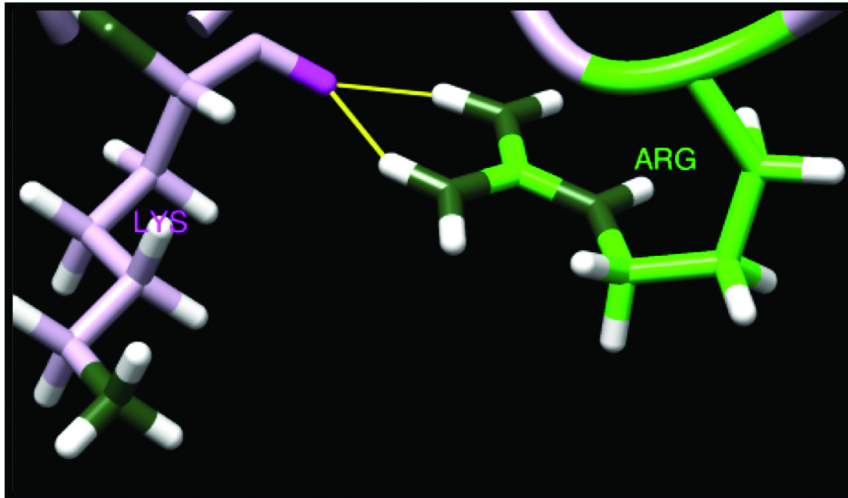


Figure S4. The hydrogen bond network of ARG213 in the WT structure model 4. The common feature is that ARG213 is either fully exposed to the water phase or makes hydrogen bonds to the neighboring backbone oxygen. The figure shows the WT structure of model 4 analyzed using the Amber force field: ARG213 (green) forms two hydrogen bonds with the backbone oxygen of neighboring residue LYS209 (light pink). The positive charge of LYS209 is far away from the side chain of ARG213.

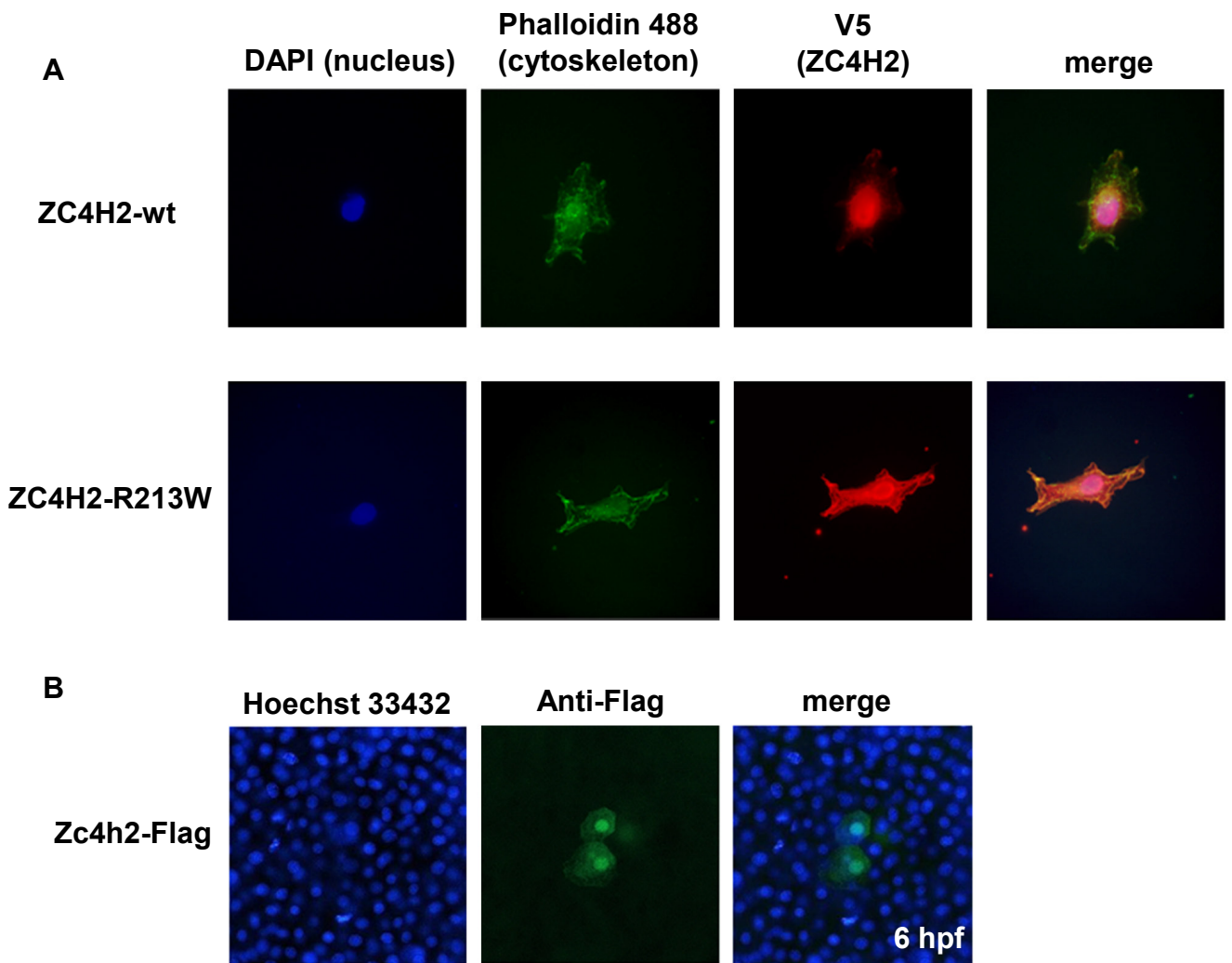


Figure S5. Subcellular localization of ZC4H2 proteins. A. Cos7-cells were transfected with a plasmid containing either *ZC4H2*-wt or the *ZC4H2*-R213W mutation. The merged signal shows the R213W mutation prevents most of the ZC4H2 protein from moving into the nucleus. Phalloidin 488 is a cytoskeleton stem and a V5 antibody was used to stain epitope-tagged *zc4h2* protein. B. *zch42*-Flag construct-injected zebrafish embryonic cells stained for anti-Flag and Hoechst 33432.

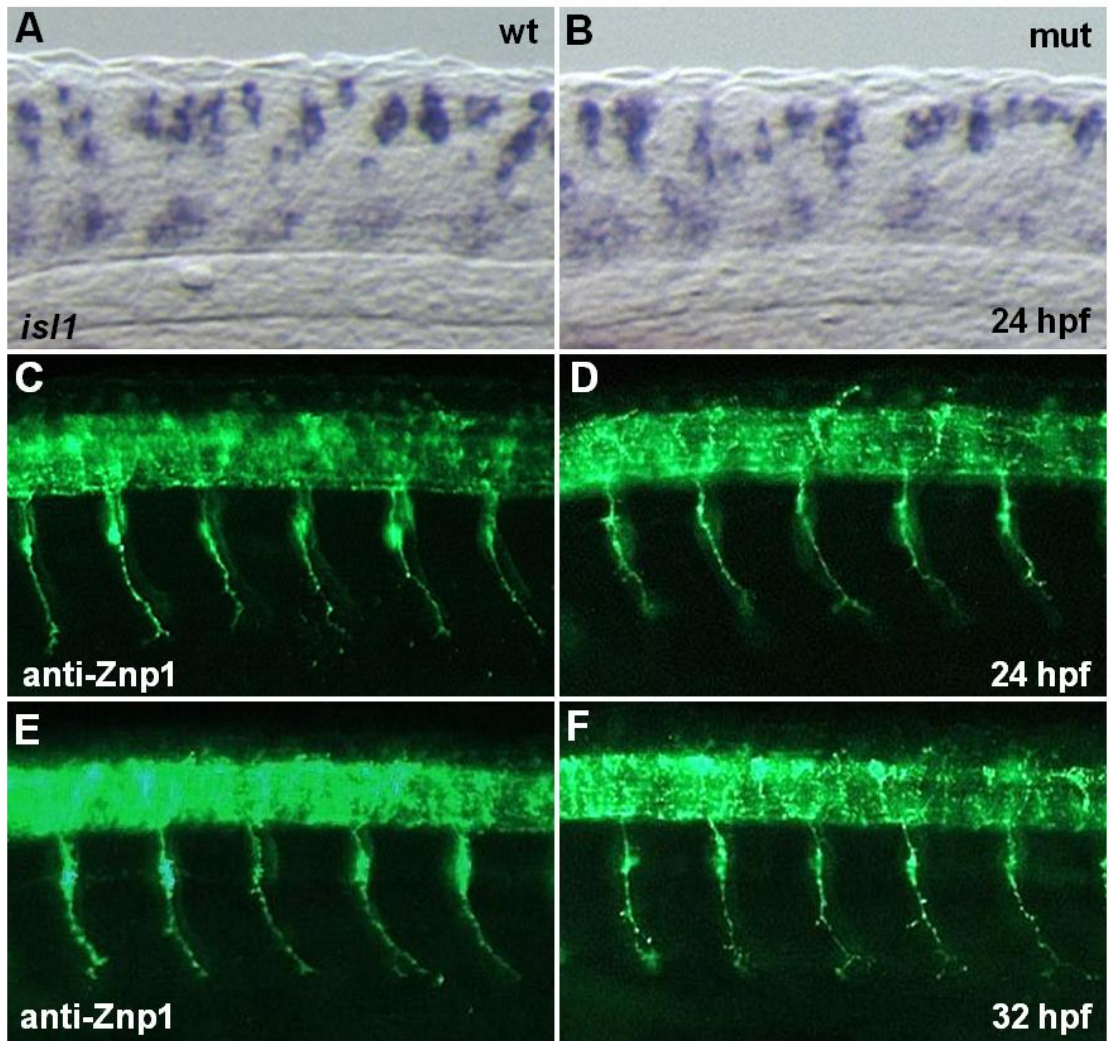


Figure S7. Whole-mount *in situ* hybridization and immunohistochemistry for markers of motoneurons in wild type sibling (wt) and *zc4h2* KO mutant (mut) embryos. A,B - Level of *isl1* transcripts, a marker for motoneurons, were not changed in the spinal cord at 24 hpf. C-F - Motoneuron projection appears normal by immunohistochemistry analysis for *znp1* at 24 and 32 hpf.

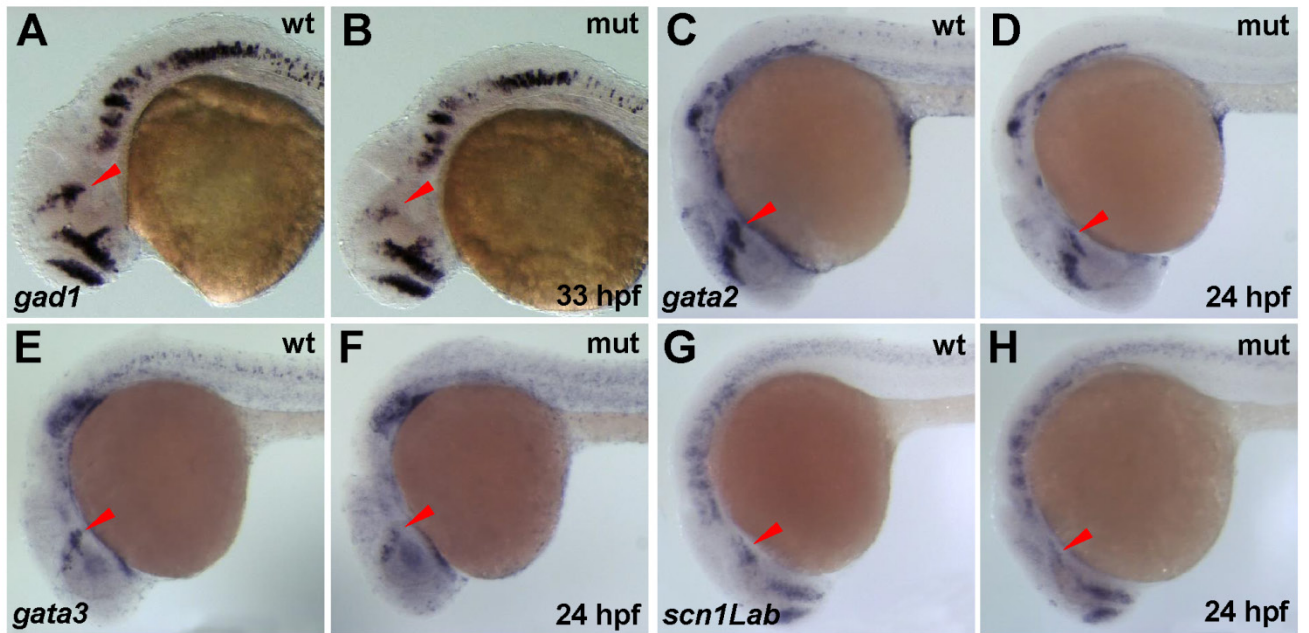


Figure S8. Whole-mount *in situ* hybridization for *gad1* at 33 hpf, and *gata2*, *gata3*, and *scn1Lab* at 24 hpf in wild type sibling (wt) and *zc4h2* mutant (mut) embryos. A,B - *gad1*, C-D. *gata2*, E-F. *gata3*, G-H. *scn1Lab* transcripts were decreased in the midbrain tegmentum of mutants (arrowhead).

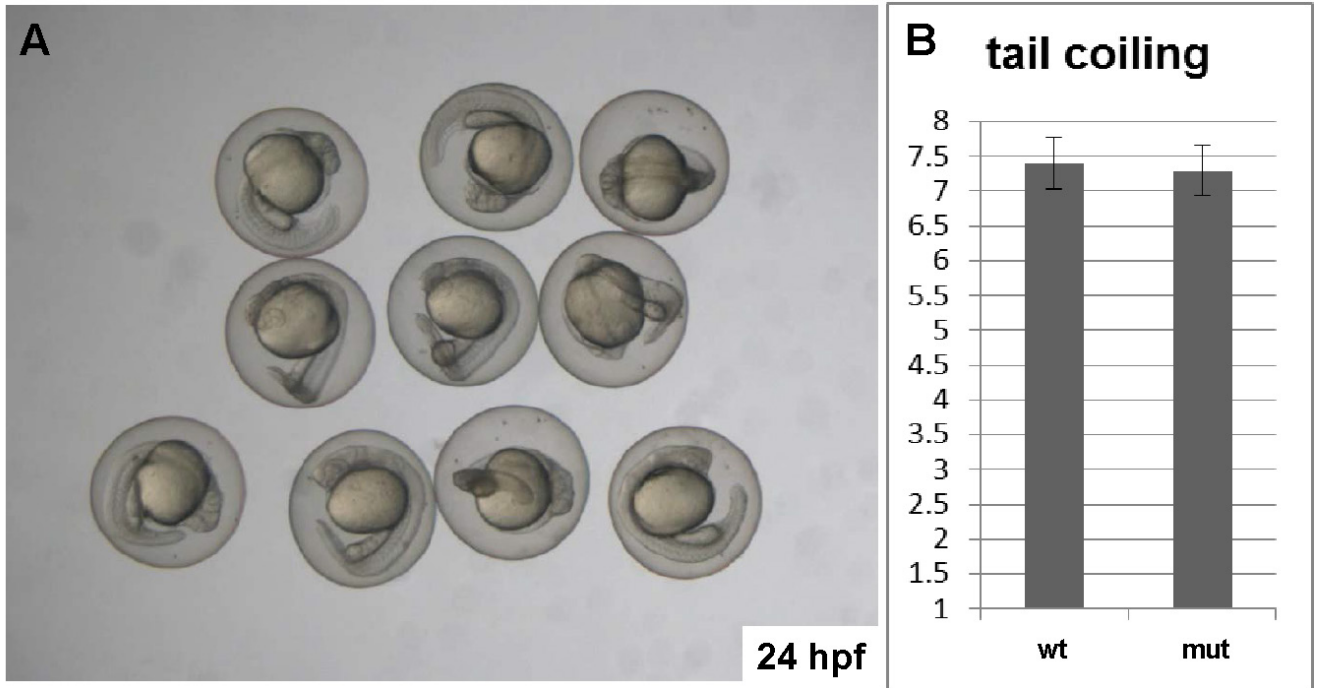


Figure S9. Analysis of tail coiling in wild type sibling (wt) and *zc4h2* KO mutant zebrafish. No detectable change was observed in tail coiling behavior of *zc4h2* mutants at 24 hpf. The frequency of tail coiling was counted per minute. Individual embryos were genotyped after counting. (n = 7 for each).

		R18K	L66H	R213W
Models Used		2, 3	5	2, 4
Eris Stability	Avg $\Delta\Delta G$	3.45	1.30	-2.036
	Stdev	0.45	N/A	15.373
FoldX Stability	Avg $\Delta\Delta G$	3.48	1.54	1.194
	Stdev	1.05	N/A	1.156
PoPMuSiC Stability	Avg $\Delta\Delta G$	0.58	1.32	0.146
	Stdev	0.62	N/A	0.286
I-Mutant2.0 Stability*	$\Delta\Delta G$	0.76	2.60	-0.09
	Stdev	N/A	N/A	N/A
PolyPhen2*	Score out of 1.000	0.979	1.000	0.999
	Damage prediction	Probably Damaging	Probably Damaging	Probably Damaging
sMMGB Stability**	Avg $\Delta\Delta G$	4.19	16.73	4.13
	Stdev	28.40	N/A	11.13
CONSENSUS PREDICTION		Mutation is Destabilizing	Mutation is Destabilizing	Mutation is Destabilizing

Table S1: Prediction results of the changes in the folding free energy of ZC4H2 as a result of point mutations. Mutations resulting in $\Delta\Delta G > 0$ are predicted to have destabilizing effects, those with $\Delta\Delta G < 0$ are predicted to have stabilizing effects.

*PolyPhen2 and I-Mutant 2.0 are primarily sequence-based predictors and return only one result per mutation and are therefore not model specific. **The results of sMMGB are shown as $-\Delta\Delta G$ to be consistent with the methodology of calculating changes in the folding free energy used by other predictors.